

Article

Synthesis and Characterizations of $(\text{Co}_x\text{Mg}_{(2-x)})\text{SiO}_4$ Forsterite Ceramic Pigments from Mirror Waste

Niti Yongvanich , Kullada Supanichwatin, Jitap Penglan and Narit Triamnak *

Department of Materials Science and Engineering, Faculty of Engineering and Industrial Technology, Silpakorn University, Nakhon Pathom 73000, Thailand; niti.yongvanich@gmail.com (N.Y.); kang.kullada@gmail.com (K.S.); chaingather_kub@hotmail.com (J.P.)

* Correspondence: triamnak_n@su.ac.th; Tel.: +66-3421-9363

Received: 10 June 2018; Accepted: 11 July 2018; Published: 13 July 2018



Abstract: Ceramic pigments have been widely used in a variety of industries because of their excellent properties, such as high thermal stability, low-cost productions, and simple manufacturing processes. Re-use of mirror waste, which consists of silicon dioxide greater than 70%, is a method that can reduce raw materials cost. In this work, ceramic pigment with forsterite structure, Mg_2SiO_4 , was synthesized via conventional solid state reaction by using mirror waste as a precursor. Solid solutions of Co-doped forsterite pigment, $\text{Co}_x\text{Mg}_{(2-x)}\text{SiO}_4$ where $x = 0.02\text{--}1.6$, were calcined at $1000\text{ }^\circ\text{C}$ for 2 h. The calcined powders were characterized by X-ray diffraction technique (XRD), Fourier-transform infrared spectroscopy (FTIR), scanning electron microscope (SEM), X-ray photoelectron spectroscopy (XPS), UV-Vis spectrophotometer, and color measurement (CIEL*a*b*). XRD results confirmed that forsterite phase was found as a main phase in the ceramic powder. However, the forsterite phase decreased with increased concentration of Co to $x = 0.8\text{--}1.6$. This could be because of the solubility limit of Co in solid solution. In addition, the use of mirror waste as a raw material was able to reduce calcination temperature compared to the use of oxide reagents. Color measurements or CIEL*a*b* color space of forsterite pigments were located in red-blue quadrant for Co-doped pigment.

Keywords: ceramic pigment; forsterite; mirror waste

1. Introduction

Ceramic pigments have been used extensively in decorative industries as a coloration component due to their advantages such as low-cost productions, stability, longevity, and mass-producibility. Even though ceramic pigments possess many advantages, the reduction of raw materials cost is still needed to compete in the market. Re-use of industrial waste is the current trend to lower the cost of raw materials. Traditionally, this waste is disposed of in landfill. It includes glass and mirror waste. The advantage of these wastes for re-use is their amorphous structure. Such structure could lead to a lower reaction temperature. However, this might cause a variation in pigment properties, such as firing formula and color tone, due to the composition differences between the waste and pure reagents. In addition, this variation could be seen between wastes of similar chemical compositions, such as glass and mirror, as well. Even though the secondary processing of glass is common, the aluminum film in mirror waste might deviate the final product properties. Practically, if the desirable pigment phase can be obtained as well as excellent chromatic quality in term of both stability and color tone, then the waste can be used. This method could be optimized and could lead to benefits both economically and environmentally.

Generally, the pigments are used as a dispersed phase in media such as glaze, ceramic body, and porcelain enamels causing the desirable color in applications. Such applications usually involve high-temperature processes. Therefore, the synthesized pigments must exhibit excellent thermal

and chemical stability. There have been researches into the synthesis, phase formation, and thermal stability in Co olivines and related compounds such as $\text{CaCoSi}_2\text{O}_6$, $\text{Ca}_2\text{CoSi}_2\text{O}_7$, and CaCoSiO_4 [1–3]. Forsterite [4,5], with the chemical formula Mg_2SiO_4 , is a crystalline magnesium silicate and seems to be usable as the ceramic pigment due to its fabulous refractoriness. It shows high thermal stability with a melting temperature of 1890 °C as well as high chemical stability. In contrast, the common way to synthesize forsterite also requires very high temperatures. It is usually fired at a temperature of approximately 1500 °C. Therefore, it is crucial to lower the synthesized temperature which also means lowering productions cost. In addition, the thermal stability of forsterite pigment needs to be investigated simultaneously to understand and optimize the pigment preparation processes.

This study aims to synthesize the forsterite pigment and characterize its properties by using mirror waste as a raw material and cobalt oxide as a chromophore of the pigment. Phase evolution and chromatic properties of the pigment are investigated with the different chromophore contents.

2. Materials and Methods

Forsterite powder was prepared via a conventional solid state reaction method by stoichiometrically mixing reagent-grade silicon dioxide (SiO_2) and magnesium oxide (MgO) as precursors. The mixture was wet ball-milled for 24 h with ethanol followed by calcination in an alumina crucible at temperatures between 800 and 1200 °C for 2 h. The as-calcined powder was then ground in a mortar prior to structural characterization by X-ray diffraction technique (XRD, LabX XRD-6100 Diffractometer, Shimadzu, Kyoto, Japan) with $\text{Cu-K}\alpha$ radiation at $\lambda = 1.5406 \text{ \AA}$. Cobalt-doped forsterite pigment ($\text{Co}_x\text{Mg}_{(2-x)}\text{SiO}_4$, when $x = 0\text{--}1.6$) was synthesized by mixing mirror waste (as the SiO_2 source) instead of reagent-grade SiO_2 , MgO and cobalt oxide (Co_2O_3), stoichiometrically. The mixed powder was subjected to the previous preparation method as the reagent grade forsterite powder. Phase evolution of the pigment powder from mirror waste was comparatively investigated by XRD technique.

Fourier transformation infrared spectroscopy (FTIR, Vertex70, Bruker, Billerica, MA, USA) was performed as a complement study for pigment structural investigation.

X-ray fluorescence (XRF, Minipal-4, PANalytical, Almelo, The Netherlands) was used to characterize mirror waste composition, as shown in Table 1. The morphology and elemental distribution of the powder were examined by scanning electron microscope (SEM, TM3030, Hitachi, Tokyo, Japan) and energy dispersive spectroscopy (EDS, TM3030, Hitachi).

Table 1. Compositions of oxides from mirror waste.

Oxides	Mol %
SiO_2	71.11
Na_2O	12.68
CaO	11.38
MgO	3.52
Etc.	1.31

Optical properties of the pigment were investigated by using the Uv-Vis spectroscopy technique (UV-1800, Shimadzu) to study light reflection character and the CIELab method by colorimeter (Color Reader CR-10, Minolta, Osaka, Japan) was used to examine chromatic values. The color is defined as the three parameters, L^* , a^* and b^* , where they represent the brightness, change from green (negative value) to red (positive value), and change from blue (negative value) to yellow (positive value), respectively.

3. Results and Discussion

The possibility of using mirror waste to synthesize forsterite pigment via the common route preparation, such as using reagent-grade SiO_2 as the precursor, needed to be investigated. Phase evolution of this composition is illustrated in Figure 1.

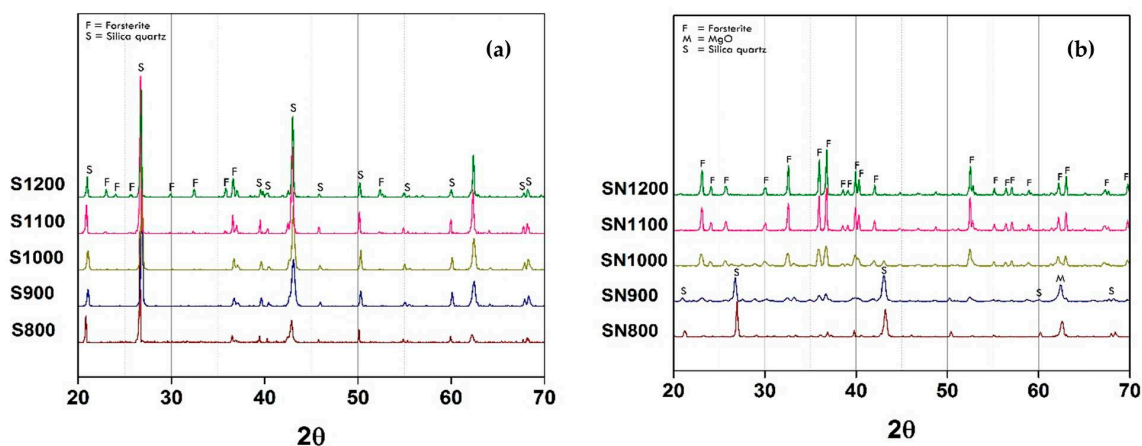


Figure 1. X-ray diffraction (XRD) patterns of as-calcined forsterite powder at various temperatures between 800 and 1200 °C by mixing reagent-grade SiO_2 : (a) Without NaF mineralizer; (b) Added 5 wt. % of NaF.

It is clearly shown in Figure 1a that the forsterite phase could not be observed even if the calcination temperature was increased to 1000 °C. With further temperature increase to 1200 °C, there was a small peak pattern of forsterite phase occurrence. On the other hand, the main phase of this powder remained as SiO_2 (labeled with “S”) which identified with JCPDF 00-046-1045. This results confirmed the difficulty of forsterite synthesis at moderate temperature by conventional solid state reaction because of its excellent refractoriness [6]. Therefore, the addition of a mineralizer, NaF, was performed to increase the raw materials diffusion rate leading to a reduction of the reaction temperature. The XRD pattern of NaF-added powder is shown in Figure 1b. Forsterite structure peaks (labeled with “F”) were observed with small intensity when the powder was calcined at temperatures as low as 800 °C which was matched to JCPDF 00-034-0189. The peak pattern intensity increased clearly when the temperature increased to 1000 °C. In addition, there was an abrupt decreased of SiO_2 precursor peaks. The single phase of forsterite structure was obtained when the calcination temperature increased up to 1100 °C. According to data in Table 1, the second highest elemental concentration of mirror waste was sodium which could play a role in forsterite formation as a similar mineralizer, NaF [6–9].

XRD pattern of as-calcined powder $\text{Co}_x\text{Mg}_{(2-x)}\text{SiO}_4$, when $x = 0$, synthesized from mirror waste are shown in Figure 2. The forsterite peaks can be clearly seen when the powder was calcined at the temperature of 800 °C, and their intensity significantly increased with the calcination temperature increase. It was observed that using mirror waste as the SiO_2 source could reduce the forsterite formation temperature [10]. This could be because of the disorder-structure within mirror waste from industrial post-processes. In addition, other oxides components, especially Na_2O , could behave as the mineralizer. It needs to be noted that the secondary phases appeared in all preparation conditions. This is because of the high impurities content in mirror waste which is very difficult to eliminate and control. However, compared to the main phase, the number of secondary phases appears to be small and influences on the pigment properties are correspondingly small.

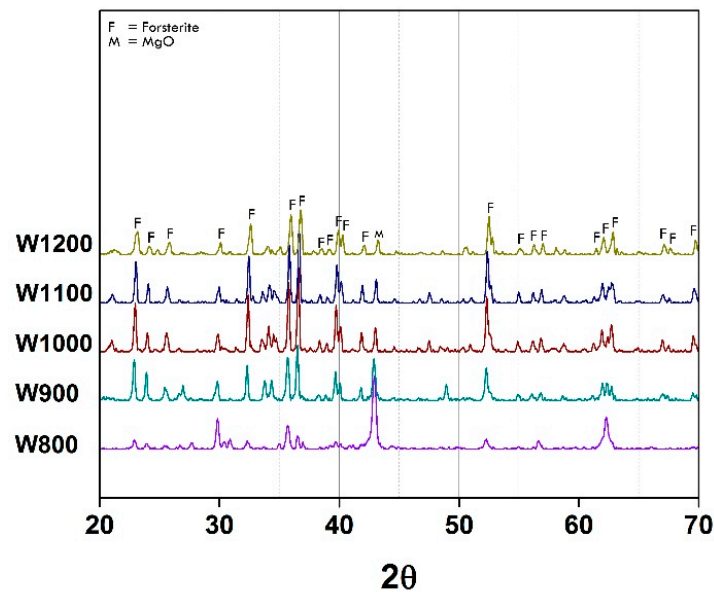


Figure 2. XRD patterns of as-calcined forsterite powder from mirror waste at various temperatures between 800 and 1200 °C.

The crystal structure characterization of forsterite mirror waste pigment with increasing concentration of Co chromophore is depicted in Figure 3. This investigation was designed to study structural stability based on the content of chromophore ion. The concentration of Co ion was varied, $x = 0-1.6$, with a constant calcination temperature of 1000 °C. This temperature was enough to obtain forsterite phase in the pigment as noted in previous XRD results. It was found that the increase of Co ion content from $x = 0$ to $x = 0.4$ caused the shifting of the peaks pattern towards a smaller diffraction angle. It could be implied that the d-spacing of unit cell increased because of the greater Co ion diffusion into the structure. The changes of unit cell volume with different Co content were observed in related compounds such as $\text{CaCoSi}_2\text{O}_6$ pyroxenes [11,12] as well. However, when the content of Co was increased to $x = 0.8-1.6$, the XRD patterns exhibit the Co_2SiO_4 phase which matched to JCPDF 00-015-0865, labeled “CS” in Figure 3d. In addition, peak intensity of this phase reduced. It might be because the excess Co interacted with the other oxides within the mixture resulting in an increase of secondary phases and decrease of the main phase [8,13].

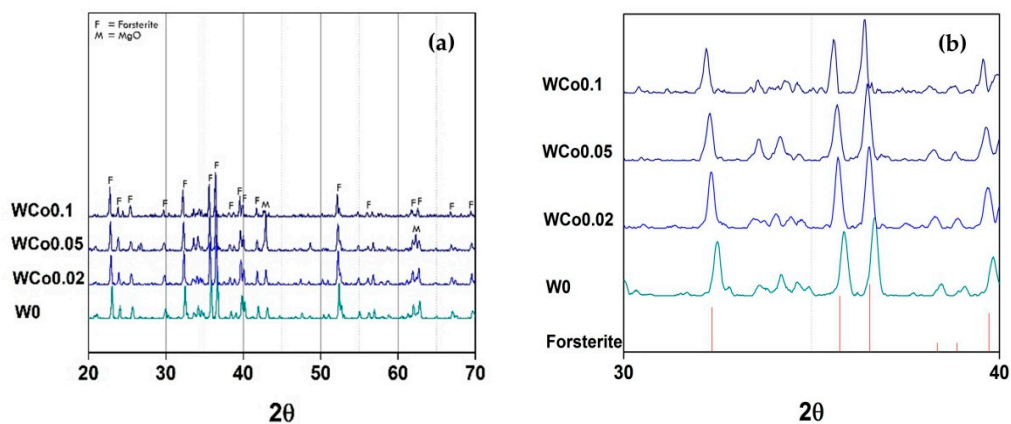


Figure 3. Cont.

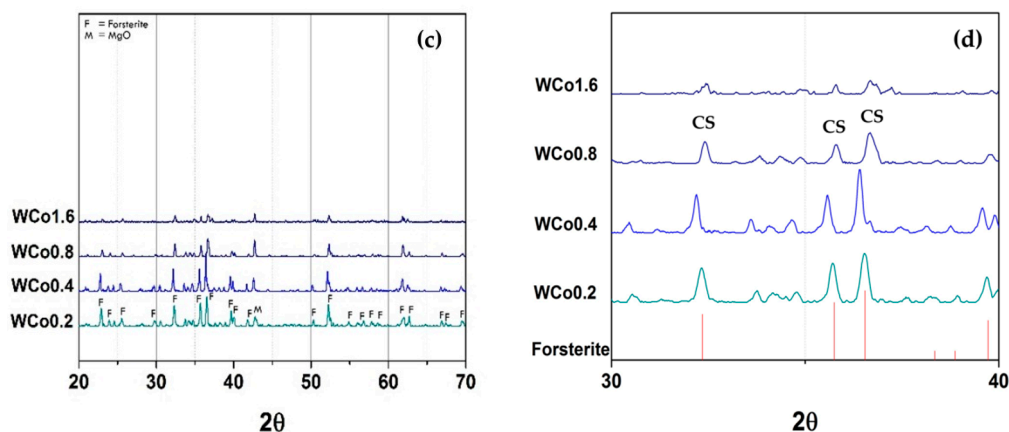


Figure 3. XRD patterns of $\text{Co}_x\text{Mg}_{(2-x)}\text{SiO}_4$ sample synthesized by mirror waste calcined at $1000\text{ }^\circ\text{C}$ for 2 h: (a,b) $x = 0\text{--}0.1$; (c,d) $x = 0.2\text{--}1.6$.

FTIR was studied as the supplementary structural characterization and is illustrated in Figure 4. The results exhibited small peaks at wave number $2800\text{--}3600\text{ cm}^{-1}$ which refer to the vibration of O-H stretching mode. These peaks were probably a result of humidity that KBr absorbed while the measurement was being conducted. In addition, the peak of O-H bending was observed at wave number of 1454 cm^{-1} which is also the evidence of water molecule existence. After that, peaks of Si-O bonding were seen at 894 and 999 cm^{-1} which are Si-O-Si stretching [14,15]. Finally, Si-O-Si bending peaks were observed at 521 and 620 cm^{-1} . As the content of Co ion increased both Si-O-Si stretching and bending peaks broadened [16]. The appearance of peak broadening was evidence of structural distortion because of the diffusion of Co ion in the structure. These results are in agreement with XRD data.

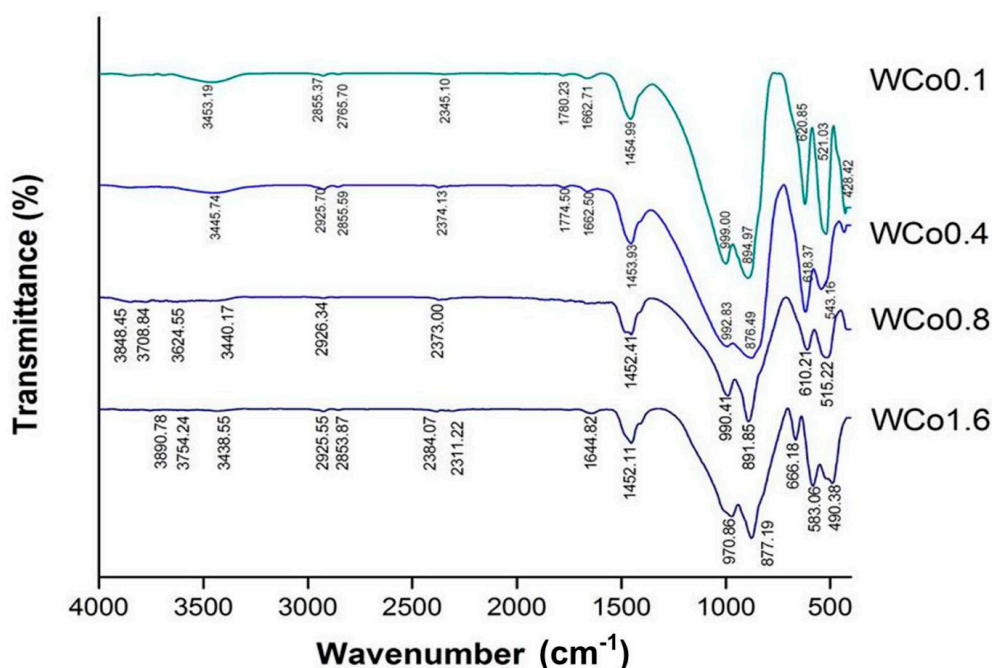


Figure 4. Fourier transformation infrared spectroscopy (FTIR) Spectrum of $\text{Co}_x\text{Mg}_{(2-x)}\text{SiO}_4$ ($x = 0.1, 0.4, 0.8, 1.6$) samples synthesized by mirror waste calcined at $1000\text{ }^\circ\text{C}$ for 2 h.

To predict the behavior of Co ion, $\text{Co}_{0.4}\text{Mg}_{1.6}\text{SiO}_4$ powder was then analyzed by X-ray photoelectron spectroscopy technique (XPS). The result of Co-2p binding energy is shown in Figure 5. It was found that there were peaks split into Co-2p_{1/2} and Co-2p_{3/2} at 797 eV and 781 eV, respectively. This result described the existence of divalent cobalt (Co^{2+}) which could mean the substitution of Co ion at the Mg position in the forsterite structure. Characterized data from XRD, FTIR, and XPS confirm that Co-doped forsterite pigment was successfully synthesized by using mirror waste as the SiO_2 source.

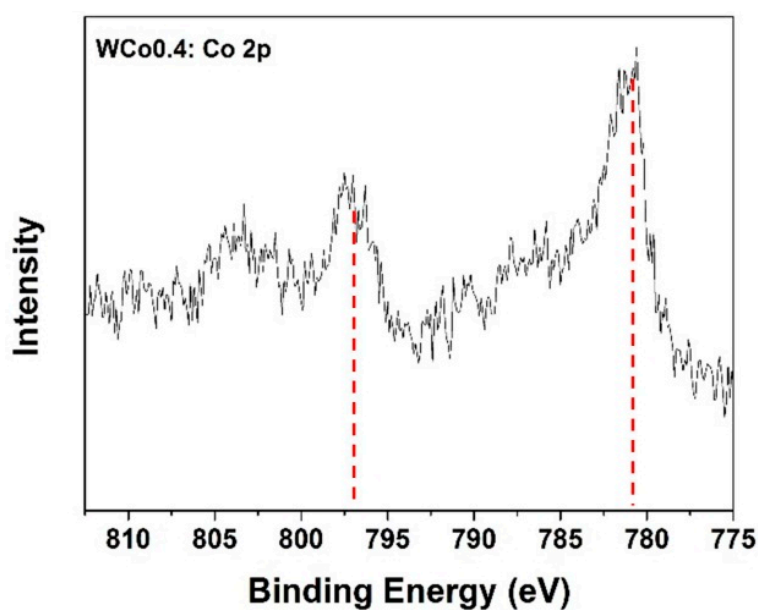


Figure 5. X-ray photoelectron spectroscopy (XPS) spectra of $\text{Co}_{0.4}\text{Mg}_{1.6}\text{SiO}_4$ samples showing binding energy of Co 2p.

The morphology and elemental distribution of the $\text{Co}_{0.4}\text{Mg}_{1.6}\text{SiO}_4$ powder obtained from SEM and EDS techniques are shown in Figure 6. It was found that the particle shape of the pigment was irregular. In addition, particle size was non-uniform. It could be a result of the non-uniformity of mirror waste structure. The majority elements of the pigment were Si and Mg as expected. Moreover, the other elements such as Co, Na and Ca were observed with small concentrations which agreed with XRF data listed in Table 1. However, distribution of Co, which was doped into the forsterite pigment, was uniform.

UV-Vis spectroscopy spectra are illustrated in Figure 7. It was found that the absorption spectra were at the wavelength of 550–700 nm. Such absorbed wavelength range is due to the excitation of electron from 4T₁(F) to 4T₁(P) and 2T₁(G) to 2T₂(G) states of Co^{2+} chromophore which located at the octahedral sites of the forsterite structure [17,18]. There are three absorption peaks in the 550–700 nm range (absorbing yellow, orange, and red). The observed color, according to the complimentary color theory, is mainly green and blue (430–560 nm) which was clearly reflected by dramatic changes in both a and b color parameters in Table 2. The a parameter remained in the redness regime whereas the b parameter displayed blueness. Upon increasing the amount of cobalt doping, slight increases in the intensity of the absorption peaks were observed as the peaks became more prominent. This phenomenon was also confirmed by an enhancement of more than double for both a and b parameters when increasing cobalt concentration from $x = 0.2$ to $x = 0.4$. This result is likely to be associated with the absence of free cobalt oxide observed by XRD and the XRD peak shift as a result of successful cobalt incorporation into the Mg lattice. As the content of Co increased to $x = 0.8$ – 1.6 , absorption strongly appeared through the full range of measured wavelength leading to dark gray color which is shown in Figure 8 [17].

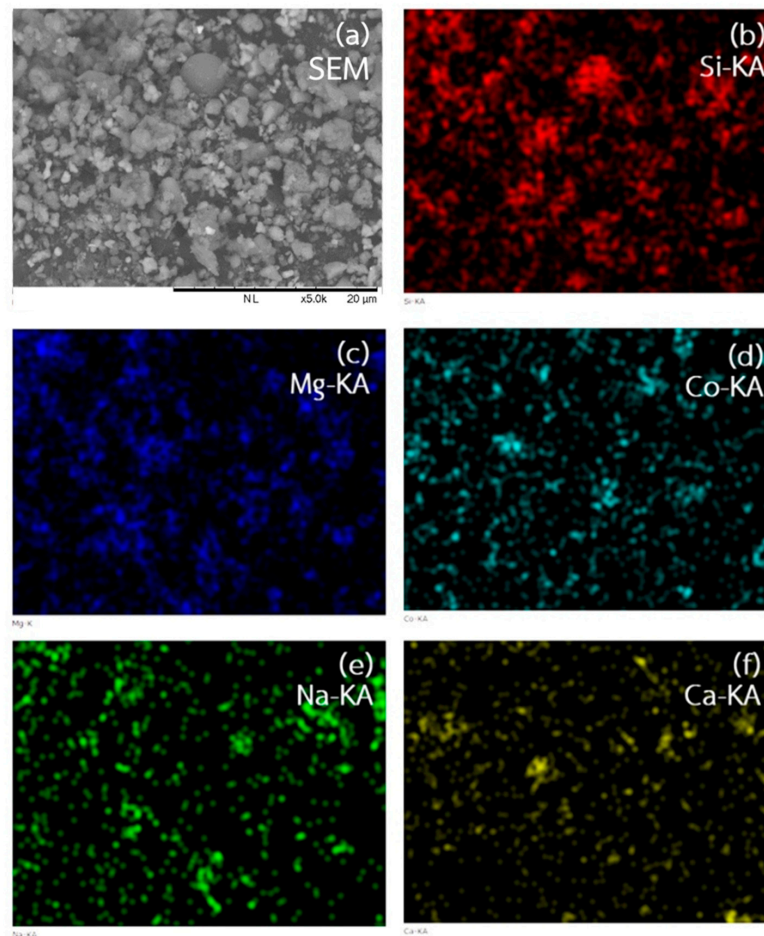


Figure 6. Scanning electron microscope (SEM) micrograph and energy dispersive spectroscopy (EDS) data of $\text{Co}_{0.4}\text{Mg}_{1.6}\text{SiO}_4$ powder: (a) morphology; (b) silicon; (c) magnesium; (d) cobalt; (e) sodium; and (f) calcium.

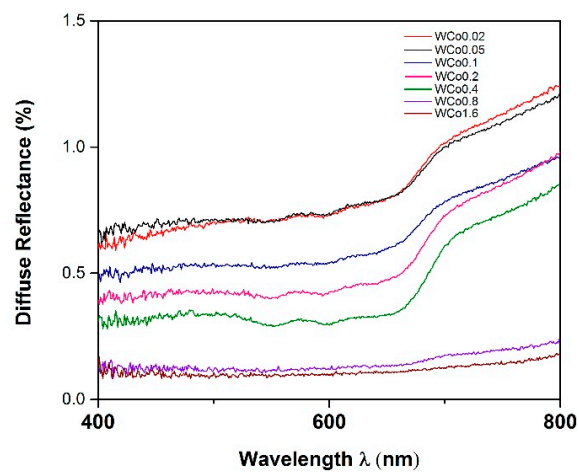
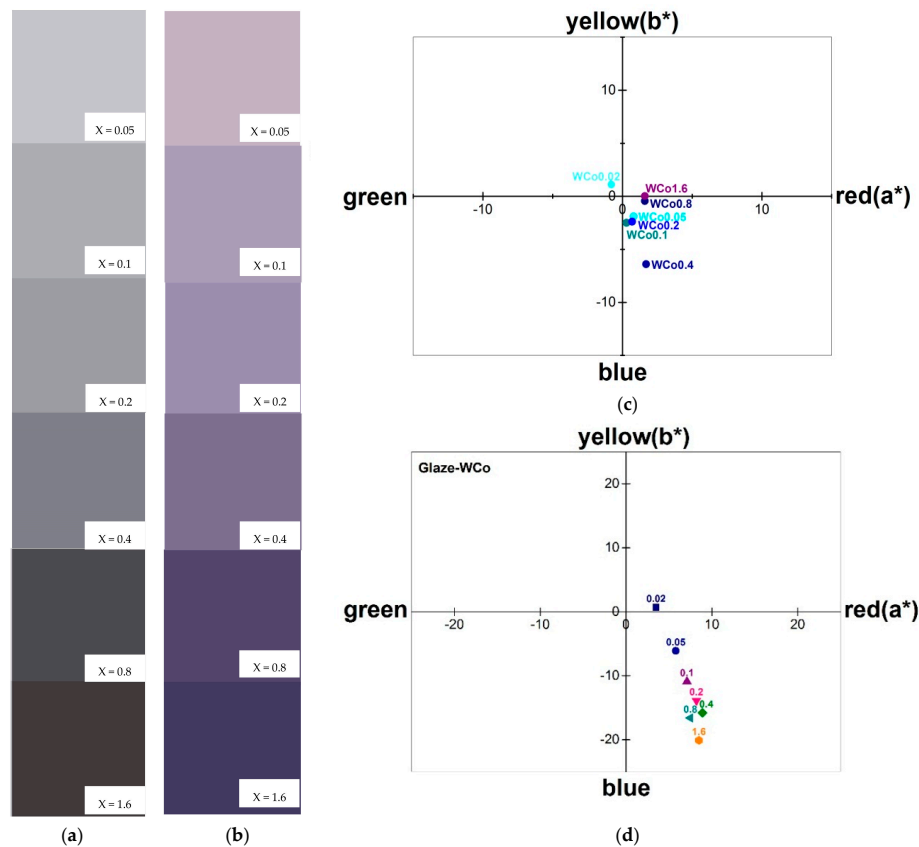


Figure 7. Diffuse reflectance spectra of $\text{Co}_x\text{Mg}_{(2-x)}\text{SiO}_4$ (where $x = 0.02\text{--}1.6$) synthesized by mirror waste calcined at $1000\text{ }^\circ\text{C}$ for 2 h.

Table 2. CIEL*a*b* data of as-calcined $\text{Co}_x\text{Mg}_{(2-x)}\text{SiO}_4$ (where $x = 0.05\text{--}1.6$) powder.

$\text{Co}_x\text{Mg}_{(2-x)}\text{SiO}_4$ (x)	L*	a*	b*
0.05	79.9	0.8	−1.9
0.1	71.1	0.3	−2.5
0.2	64	0.7	−2.4
0.4	52.9	1.7	−6.4
0.8	32.8	1.6	−1.8
1.6	25.5	1.6	−0.1

**Figure 8.** Chromatic tone and CIEL*a*b* diagram of $\text{Co}_x\text{Mg}_{(2-x)}\text{SiO}_4$ (where $x = 0.05\text{--}1.6$): (a,c) As-calcined powder; (b,d) Mixing glaze fired powder.

Chromatic characteristics of $\text{Co}_x\text{Mg}_{(2-x)}\text{SiO}_4$ with various content of Co are illustrated in Figure 8. Parameters L^* , a^* and b^* , which were measured by CIELab method, are listed in Table 2. Brightness, L^* , decreased as the Co content increased leading to a darker tone and was seen in the similar trend of UV-Vis spectra. In addition, $\text{Co}_x\text{Mg}_{(2-x)}\text{SiO}_4$ pigments tended to exhibit their color in positive a^* and negative b^* coordination as shown in Figure 8b which showed violetish color [19,20]. As pigment application is generally dispersed in glaze, its glazed chromatic properties were investigated and are shown in Figure 8b,d. Pigments were mixed with low-temperature glaze powder (1000 °C firing glaze) with 10:90 wt. % ratio and followed by firing at 1000 °C for 2 h. After firing, the mixtures were ground to a fine powder before color measurement. It was found that the color of the mixtures changed and exhibited more violetish than as-calcined pigments as shown in Figure 8a,c. The parameters a^* and b^* showed a greater value in the identical quadrantal coordination as shown in Figure 8d. The differences in pigment color quality are listed in Table 3 which are calculated by an equation as follows:

$$dE^* = \sqrt{dL^{*2} + da^{*2} + db^{*2}} \quad (1)$$

where dE^* identified as the color stability of the pigments after glaze which is calculated from the differences of the L^* , a^* , and b^* parameters from prior to and after being glazed. Generally, the acceptable value of dE^* should be less than 1. It was discovered that the calculated value of the pigments was greater than 1 in every doping compositions, shown in Table 3. The unsteady color changes also tend to increase as the Co content increased. It is probably because of the excess Co ions' outward diffusion from the forsterite pigments. This prediction was confirmed by the EDS results which are depicted in Figure 9. The interface between as-calcined powder and low-temperature glaze powder (CG466) was created by cold isostatic compression to pellet form. Then it was subjected to the identical temperature profile as previous procedures. The elements existences at the interfacial vicinity were then investigated by EDS technique and are illustrated in Figure 9. It is clearly seen that Co ion diffused and leaked from the pigment region and spread homogeneously across the interface. The ready dissolution of Co was the origin of color changes of the pigments and exhibited insufficient stability within the glaze. This instability might be improved by further investigations, such as temperature profile adjustment in processing or co-dopings into the pigments.

Table 3. Color stability dE^* of $\text{Co}_x\text{Mg}_{(2-x)}\text{SiO}_4$ (where $x = 0.05\text{--}1.6$) pigments after being glazed.

$\text{Co}_x\text{Mg}_{(2-x)}\text{SiO}_4$ (x)	dE^*
0.05	8.6
0.1	11.8
0.2	14.1
0.4	12.4
0.8	15.9
1.6	21.3

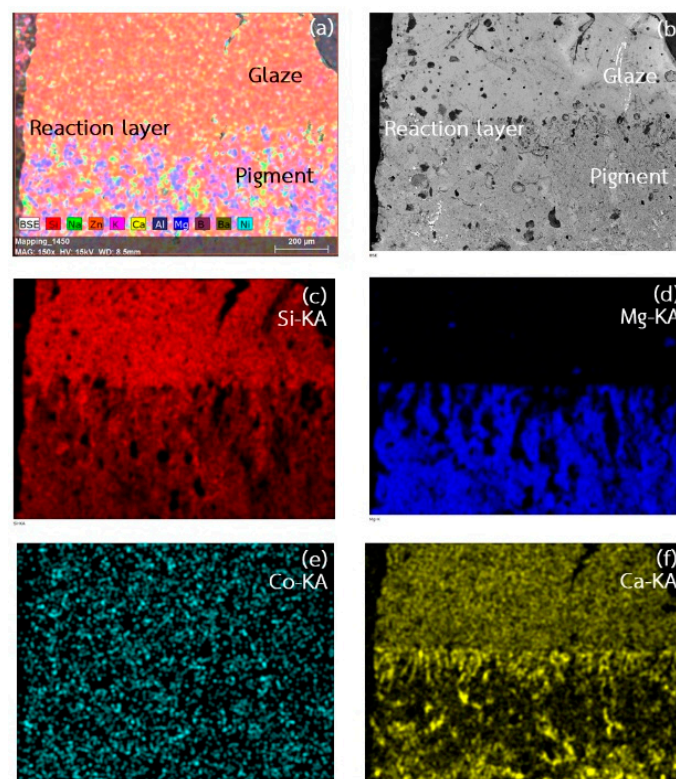


Figure 9. EDS mapping of the interface between $\text{Co}_{0.1}\text{Mg}_{1.9}\text{SiO}_4$ pigment and low-temperature glaze: (a) existing elements; (b) morphology of inter-layer between pigment and glaze; (c) silicon; (d) magnesium; (e) cobalt; and (f) calcium.

4. Conclusions

The pigments with Co-doped forsterite structure were successfully synthesized from mirror waste. The phase evolution of the pigments was investigated, and it was found that mirror waste could decrease the calcination temperature. It was because of the other oxides within mirror waste, such as Na₂O. FTIR and XPS measurements confirmed the existence of Co²⁺ ion in the pigment structure. The Co doping caused the forsterite pigment to color violetish. Color tone was darker as the concentration of doping ion increased which was illustrated by UV-Vis spectroscopy and the CIELab method. However, the forsterite pigments showed low stability in glaze which was because of the diffusion of Co chromophore. The stability of this mirror waste pigment could be enhanced by further investigation.

Author Contributions: N.T. planned the experimental activities, performed the data analysis and interpretation, and wrote the paper. N.Y. planned the experimental activities, supported raw materials, and interpreted the results of the color characterizations. K.S. and J.P. performed the materials synthesis and structural characterizations.

Funding: This research was funded by Silpakorn University Research and Development Institute (Fiscal Year 2017).

Acknowledgments: The authors also would like to acknowledge the Department of Materials Science and Engineering, Faculty of Engineering and Industrial Technology, Silpakorn University.

Conflicts of Interest: The authors declare no conflict of interest.

References

1. Mukhopadhyay, S.; Jacob, K. Phase Equilibria in the System CaO-CoO-SiO₂ and Gibbs Energies of Formation of the Quaternary Oxides CaCoSi₂O₆, Ca₂CoSi₂O₇, and CaCoSiO₄. *Am. Mineral.* **1996**, *81*, 963–972. [[CrossRef](#)]
2. Mimani, T.; Ghosh, S. Combustion synthesis of cobalt pigments: Blue and pink. *Curr. Sci.* **2000**, *78*, 892–896.
3. Navrotsky, A.; Coons, W.E. Thermochemistry of some pyroxenes and related compounds. *Geochim. Cosmochim. Acta* **1976**, *40*, 1281–1288. [[CrossRef](#)]
4. Svryru, J.R.; Inp RonBnt, M.H. The Crystal Structures of Forsterite and Horttonolite at Several Temperatures Up to 900°C. *Am. Mineral.* **1973**, *58*, 588–593.
5. Hazen, R. Effects of temperature and pressure on the crystal structure of forsterite. *Am. Mineral.* **1976**, *61*, 1280–1293.
6. Cheng, L.; Liu, P.; Chen, X.; Niu, W.; Yao, G.; Liu, C.; Zhao, X.; Liu, Q.; Zhang, H. Fabrication of nanopowders by high energy ball milling and low temperature sintering of Mg₂SiO₄ microwave dielectrics. *J. Alloys Compd.* **2012**, *513*, 373–377. [[CrossRef](#)]
7. Sedel'nikova, M.B.; Pogrebenkov, V.M.; Liseenko, N.V. Effect of mineralizers on the synthesis of ceramic pigments from talc. *Glass Ceram.* **2009**, *66*, 223–226. [[CrossRef](#)]
8. El Hadri, M.; Ahamdane, H.; El Idrissi Raghni, M.A. Sol gel synthesis of forsterite, M-doped forsterite (M=Ni, Co) solid solutions and their use as ceramic pigments. *J. Eur. Ceram. Soc.* **2015**, *35*, 765–777. [[CrossRef](#)]
9. Tavangarian, F.; Emadi, R. Synthesis of nanocrystalline forsterite (Mg₂SiO₄) powder by combined mechanical activation and thermal treatment. *Mater. Res. Bull.* **2010**, *45*, 388–391. [[CrossRef](#)]
10. Esteves, D.; Hajjaji, W.; Seabra, M.P.; Labrincha, J.A. Use of industrial wastes in the formulation of olivine green pigments. *J. Eur. Ceram. Soc.* **2010**, *30*, 3079–3085. [[CrossRef](#)]
11. Mantovani, L.; Tribaudino, M.; Dondi, M.; Zanelli, C. Synthesis and color performance of CaCoSi₂O₆ pyroxene, a new ceramic colorant. *Dyes Pigment* **2015**, *120*, 118–125. [[CrossRef](#)]
12. Gori, C.; Tribaudino, M.; Mantovani, L.; Gatta, G.D.; Delmonte, D.; Gilioli, E.; Mezzadri, F.; Calestani, G. Synthesis and crystal structure of C_{2/c} Ca(Co,Mg)Si₂O₆ pyroxenes: Effect of the cation substitution on cell volume. *Mineral. Mag.* **2017**, *81*, 1129–1139. [[CrossRef](#)]
13. Ianoş, R.; Lazău, R. Chromium-doped calcium zirconate—A potential red shade pigment: Preparation, characterization and testing. *Dyes Pigment* **2014**, *105*, 152–156. [[CrossRef](#)]

14. Eliziário, S.A.; de Andrade, J.M.; Lima, S.J.G.; Paskocimas, C.A.; Soledade, L.E.B.; Hammer, P.; Longo, E.; Souza, A.G.; Santos, I.M.G. Black and green pigments based on chromium–cobalt spinels. *Mater. Chem. Phys.* **2011**, *129*, 619–624. [[CrossRef](#)]
15. Kharaziha, M.; Fathi, M.H. Synthesis and characterization of bioactive forsterite nanopowder. *Ceram. Int.* **2009**, *35*, 2449–2454. [[CrossRef](#)]
16. López-Navarrete, E.; González-Elipe, A.R.; Ocaña, M. Non-conventional synthesis of Cr-doped SnO₂ pigments. *Ceram. Int.* **2003**, *29*, 385–392. [[CrossRef](#)]
17. Llusar, M.; Forés, A.; Badenes, J.A.; Calbo, J.; Tena, M.A.; Monrós, G. Colour analysis of some cobalt-based blue pigments. *J. Eur. Ceram. Soc.* **2001**, *21*, 1121–1130. [[CrossRef](#)]
18. Leite, A.; Costa, G.; Hajjaji, W.; Ribeiro, M.J.; Seabra, M.P.; Labrincha, J.A. Blue cobalt doped-hibonite pigments prepared from industrial sludges: Formulation and characterization. *Dyes Pigment* **2009**, *81*, 211–217. [[CrossRef](#)]
19. Maslennikova, G.N.; Pishch, I.V.; Radion, E.V. Current classification of ceramic silicate pigments. *Glass Ceram.* **2006**, *63*, 281–284. [[CrossRef](#)]
20. Pogrebenkov, V.M.; Sedel'nikova, M.B.; Vereshchagin, V.I. Talc-based ceramic pigments. *Glass Ceram.* **1997**, *54*, 351–353. [[CrossRef](#)]



© 2018 by the authors. Licensee MDPI, Basel, Switzerland. This article is an open access article distributed under the terms and conditions of the Creative Commons Attribution (CC BY) license (<http://creativecommons.org/licenses/by/4.0/>).